Closely related facultative and constitutive CAM phenotypes show little transcriptomic overlap in the subgenus *Tillandsia*

Clara Groot Crego[1,2], Sarah Saadain[1,2,3], Marylaure De La Harpe[1], Jacqueline Hess[1,4], Michael H.J. Barfuss[1], Walter Till[1], Christian Lexer[1,†], Ovidiu Paun[1]

[1]Department of Botany and Biodiversity Research, University of Vienna, 1030 Vienna, Austria
[2]Vienna Graduate School of Population Genetics, Vienna, Austria
[3]Institut für Populationsgenetik, Vetmeduni Vienna, 1210 Vienna, Austria
[4]Cambrium GmbH, Max-Urich-Str. 3, 13055 Berlin, Germany

[†]deceased

Correspondence to: clara.groot.crego@univie.ac.at, ORCID: 0000-0002-4547-3608

Word count for Introduction: **1,057**
Word count for Methods: **2,022**
Word count for Results: **2,571**
Word count for Discussion: **1,263**
Word count for Conclusion**: 234**
Word count for main body: 7,147
Number of Figures: **7**
Number of Tables: **0**
Number of SI: **6 figures, 8 tables**

1. Summary

- The evolutionary trajectory of Crassulacean acid metabolism (CAM) remains elusive, as it has evolved repeatedly, yet represents a complex trait requiring changes on several organismal levels. It is debated whether distinct forms of CAM embody a single quantitative trait, or entirely separate, categorical phenotypes. The subgenus *Tillandsia* provides an excellent opportunity to compare the genetic basis of different forms of CAM, as species are closely related, yet display a broad range of CAM phenotypes.
- By combining physiological and transcriptomic analyses of well-watered and drought-stressed accessions of a *Tillandsia* species pair, we achieved a comprehensive characterization of their photosynthetic phenotypes and the transcriptomic underpinnings and overlap of distinct CAM phenotypes in *Tillandsia*.
- We found that a species previously identified as C3 displays an active CAM cycle under drought stress, yet the effect of drought was markedly increased compared to the constitutive CAM species . The CAM-specific transcriptomic response to day-night changes and to drought showed little overlap between the two species, with most DE genes showing distinct regulation patterns or being unique to one species.
- Our study reveals that the two species do not exhibit a shared transcriptomic basis of CAM expressed at distinct levels, but that different transcriptomic routes can lead to similar phenotypes, supporting the view that CAM is a highly polygenic trait.

Key words: Crassulacean acid metabolism, drought tolerance, genetic redundancy, transcriptomics, Bromeliaceae, adaptive radiation, key innovation trait

2. Introduction

The repeated evolution of complex traits has been a long-standing matter of study for evolutionary biologists. Although one can anticipate that traits governed by a single mutation arise regularly during the course of evolution, it remains puzzling how some complex traits, necessitating alterations across multiple organismal layers, have evolved frequently and repeatedly across the tree of life.

One explanation for this is that similar phenotypes can be obtained through different underlying sets of mutations, also referred to as "genetic routes", assuming complex traits are highly polygenic and the underlying genes show a significant level of redundancy (Goldstein and Holsinger, 1992; Nowak *et al.*, 1997; Barghi, Hermisson and Schlötterer, 2020; Láruson, Yeaman and Lotterhos, 2020). Indeed, instances where similar phenotypes have evolved without a common genetic basis have been observed across a broad spectrum of life including beach mice (Steiner *et al.*, 2009), conifers (Yeaman *et al.*, 2016), lab-reared *Drosophila* (Barghi *et al.*, 2019) and cacao plants. (Hämälä *et al.*, 2020)

An example of a complex but highly evolvable trait is Crassulacean Acid Metabolism (CAM), a carbon-concentrating mechanism that has evolved independently in at least 38 plant families, amounting to a minimum of 66 independent origins (Gilman *et al.*, 2023). CAM plants restructure part of the photosynthetic metabolism across the diel cycle by assimilating CO_2 at night, rather than during the day as C3 plants do. A key difference between CAM and C3 plants is that CO_2 is temporarily converted to malate by phosphoenolpyruvate carboxylase (PEPC). The malate is stored in the vacuole overnight, and reconverted to CO_2 during the day for the Calvin Benson cycle. The CO_2 accumulated overnight allows the plant to close its stomata during the day, which has two effects: it increases the cellular concentration of CO_2 compared to O_2 in the cell, making Rubisco more efficient (Osmond, 1978), and it significantly decreases daytime evapotranspiration, increasing the plants' water use efficiency (Borland *et al.*, 2014). This is especially beneficial under high temperature or drought-stress conditions, which increase Rubisco's oxygenation activity (Heyduk, Ray and Leebens-Mack, 2021).

CAM has long been considered a complex trait, not only because of the concerted changes of temporal expression required to set the alternate biochemical pathway in motion, but also because certain anatomical features appear associated with CAM and may therefore be required for a plant to express CAM to its fullest (Nelson, Sage and Sage, 2005). Examples of such

86 anatomical features are larger vacuoles (Heyduk *et al.*, 2016; Males, 2018), tighter cell packaging
87 (Nelson and Sage, 2008) and succulence (Gibson, 1982; Griffiths *et al.*, 2008), but see (Martin,
88 Hsu and Lin, 2009).

89 Initially, CAM was regarded as a discrete trait with a bi-modal distribution of phenotypes
90 (a plant is either C3 or CAM), in part because the main method of measuring CAM activity using
91 carbon isotope measurements lacks sensitivity to detect intermediate forms (Pierce, Winter and
92 Griffiths, 2002; Winter and Holtum, 2002). In the meantime, other methods of measuring CAM
93 activity have revealed the existence of many intermediate forms, which show that at least low-
94 level or episodic expression of CAM can occur without major anatomical changes (Silvera,
95 Santiago and Winter, 2005; Heyduk, Ray and Leebens-Mack, 2021). These findings have caused
96 a shift towards thinking of CAM as a continuum. However, there exists a discrepancy between the
97 idea of CAM being a continuous trait ranging from not being expressed at all to being fully
98 expressed, and the many 'types' of CAM that have been described in the literature (e.g. "facultative
99 CAM", "weak CAM", "CAM-cycling", "strong CAM", "constitutive CAM", etc.) which are not
100 consistent with an ordered set of continuous phenotypes (Edwards, 2023).

101 It is, in other words, still unclear whether CAM is in fact a complex trait that can be
102 achieved by multiple routes of adaptation, or a true continuous trait with a shared genetic basis
103 that is expressed to different degrees among plant species. Comparative genetic analyses between
104 different CAM phenotypes help understand to what degree CAM evolution has a constrained
105 evolutionary path or a large genetic redundancy with multiple genetic routes to achieve similar
106 phenotypic outcomes. For example, Heyduk *et al.* (2018) found both shared and variable patterns
107 of gene expression in CAM-related genes among members of the Agavoideae with weak and
108 strong CAM phenotypes. More studies on the molecular basis of CAM on closely related taxa
109 expressing distinct CAM phenotypes are needed to obtain a comprehensive view of CAM
110 evolution.

111 The subgenus *Tillandsia* (genus *Tillandsia*, Bromeliaceae) is an emerging model to study
112 repeated evolution of ecological traits within a plant adaptive radiation. As part of one of the fastest
113 diversifying lineages in the plant kingdom (Givnish *et al.*, 2014), the subgenus is considered an
114 adaptive radiation that generated more than 250 species over the last 7 million years (Barfuss *et*
115 *al.*, 2016; Mendoza *et al.*, 2017; Yardeni *et al.*, 2023). Numerous key innovation traits characterise

116 this radiation, including CAM, which occurs in a broad range of phenotypes ranging from C3-like
117 to constitutive CAM (Crayn, Winter and Smith, 2004; De La Harpe *et al.*, 2020).
118 In this study, we test whether facultative and constitutive CAM species have a shared
119 genetic basis that is expressed at different levels - suggesting that CAM is a continuous trait - or,
120 alternatively, achieve CAM by distinct genetic routes. We subjected plants to experimental
121 drought stress followed by physiological and transcriptomic analyses contrasting the
122 photosynthetic phenotypes of two *Tillandsia* species. The species in question, *T. leiboldiana* and
123 *T. vanhyningii* (originally *T. ionantha var. vanhyningii*, recently reassigned to species level by
124 Beutelspacher & Garcia-Martinez (2021)), display some of the most disparate carbon isotope
125 measurements in the group (De La Harpe et al. 2020). *T. leiboldiana'*s photosynthetic phenotype
126 was studied in depth in standard conditions by a recent study using metabolomic, comparative
127 genomic and transcriptomic analyses (Groot Crego *et al.*, 2024), which revealed CAM-like
128 expression profiles of relevant genes, yet a C3-like phenotype. This led to the suggestion that it
129 may be a facultative CAM plant that performs a C3 cycle in normal conditions but might have the
130 ability to activate a weak CAM cycle, for example under drought conditions. Our study describes
131 the photosynthetic phenotypes of these *Tillandsia* species in unprecedented detail and elucidate
132 the extent of drought tolerance of different CAM phenotypes. Our analyses reveal a lack of overlap
133 between species in the transcriptomic response of CAM-related genes to both day-night changes
134 and to drought, despite both displaying CAM under drought conditions.
135

136 **3. Material and Methods**

137 **3.1. Experimental set-up and sampling**

138 We designed an experiment that captures both CAM-related and drought-stress-related
139 changes in physiology and gene expression. For this, two species of the subgenus *Tillandsia* were
140 selected: *T. vanhyningii* and *T. leiboldiana*. While reported carbon isotope ratios classify *T.*
141 *vanhyningii* as a strong and constitutive CAM plant ($\delta^{13}C$ = -13.9, (De La Harpe *et al.*, 2020)), and
142 *T. leiboldiana* as a C3 plant ($\delta^{13}C$ = -31.3), the close relatedness of the two lineages within a clade
143 known for multiple C3/CAM switches makes it likely that previously reported C3 species may in
144 fact be intermediate CAM/C3 performing weak CAM, CAM idling or facultative CAM. Features
145 of *T. leiboldiana*'s phenotype uncovered by (Groot Crego *et al.*, 2024) further indicate that it may
146 be able to perform some form of weak CAM. We therefore designed an experimental set-up that
147 tests the respective phenotypes of both species in normal and drought-stress conditions.

148 The experiment comprised six clonal accessions per species (Table S1), which were placed
149 under identical greenhouse conditions in October 2018 at the greenhouse facilities of the Botanical
150 Garden of the University of Vienna. Prior to the experiment, the accessions were allowed to
151 acclimate to greenhouse conditions for 6 weeks, before being placed in a regime of 12 hours of
152 light / 12 hours of dark for 14 days, by complementing daylight with artificial growing lights.
153 During this time, three accessions of each species were placed in a drought regime for 14 days by
154 not watering. The remaining three accessions were kept in normal watering conditions used to
155 maintain the plants in the botanical garden (1x every two days, control). After 14 days, all
156 accessions were sampled every 6 hours (Four timepoints: Day + 4 hours (10 am), Day + 10 hours
157 (4 pm), Night + 4 hours (10 pm), Night +10 hours (4 am)), generating three replicates for the
158 combination of treatments (species x time point x watering regime (Fig. 1). To minimise
159 wounding, leaf material was collected at each timepoint by delicately pulling out an entire leaf
160 from the base of the plant. The tip and base of the leaf were then removed, and the middle part was
161 immediately placed in liquid nitrogen and stored at -80 °C.

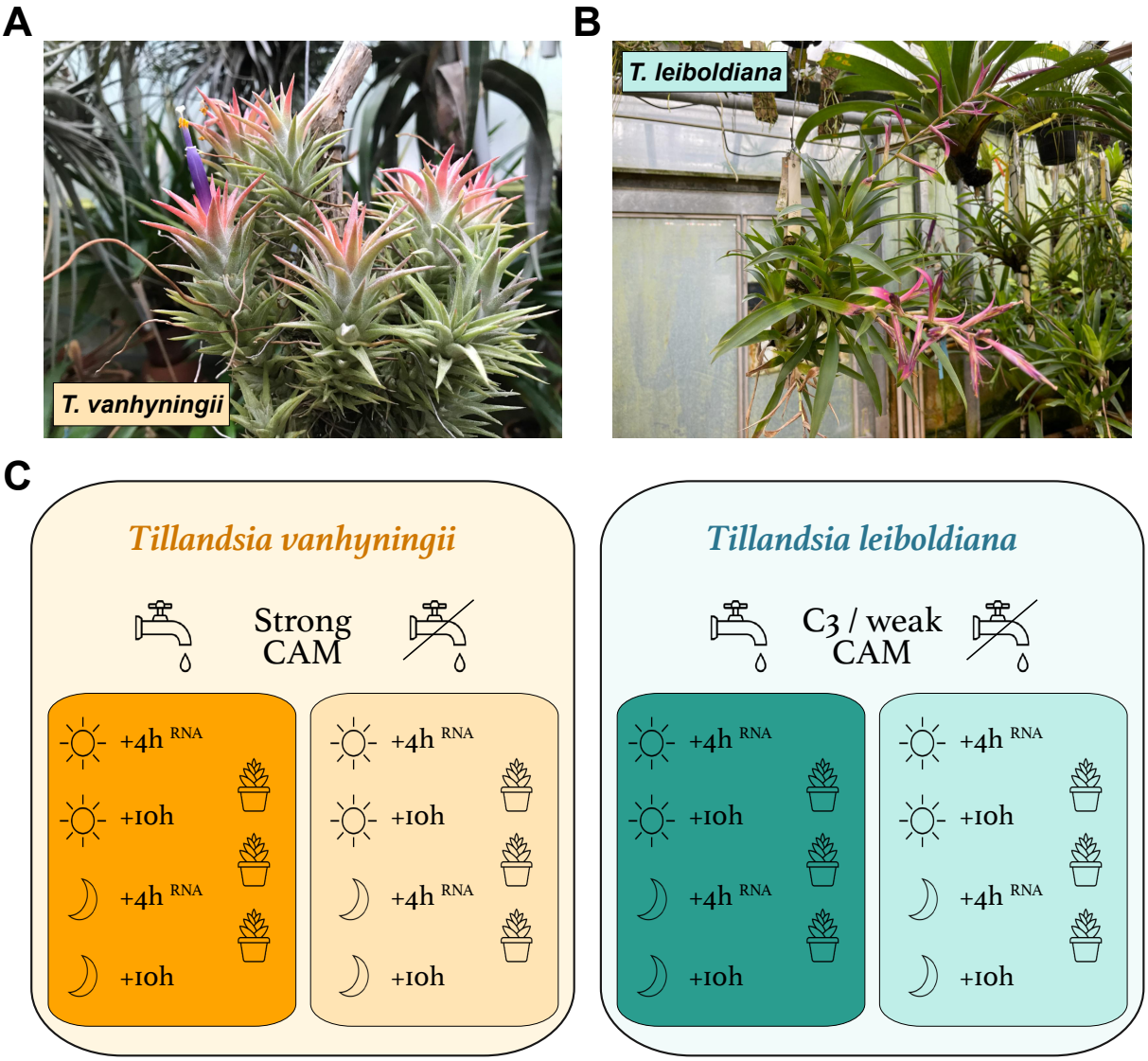

Figure 1. ***A)*** *Accession of* Tillandsia leiboldiana *at the Botanical Garden of the University of Vienna (Photograph by Michael H.J. Barfuss, 2023).* ***B)*** *Accession of Tillandsia vanhyningii at the Botanical Garden of the University of Vienna (Photograph by Manuel Lasserus, 2024).* ***C)*** *Experimental setup, consisting of six clonal accessions per species, of which three specimens are used per watering treatment, sampled at four time points, resulting in three samples per species, time point and treatment. Titratable acidity was quantified for each condition, whereas RNA-seq data was analysed for the time points indicated with* ^{RNA}.

170 ### 3.2. Titratable acidity measurements

171 Frozen leaf material for all four timepoints, two watering regimes and two species (48
172 samples in total) was weighed and then ground in a pre-cooled mortar to a powder, then added to
173 a 5 ml solution of 80 % EtOH. The samples were then incubated for one hour in an 80 °C water
174 bath with occasional vortexing. Tubes were centrifuged at 5,000 rpm for 5 minutes, after which
175 the supernatant was transferred and the pellet discarded. The extractions were then let to cool to
176 room temperature. Using a pH526 WTM Sentix mic metre, each sample was measured by titrating
177 0.1 N NaOH to the solution until reaching a pH of 8.2 exactly and recording the volume of added
178 NaOH. Titratable acidity (TA) in µ-equivalents per gram of fresh weight (g FW) was calculated
179 as µl NaOH x 0.1 mol/L/g FW.

180 To test whether titratable acidity significantly fluctuated across time within each species
181 and watering regime, we constructed a Linear Mixed-Effects Model (LMM) for each species as
182 follows:

183 $$titratable\ acid \sim watering\ regime\ \times\ time\ point\ +\ (\ 1\ |\ replicate\ )$$

184 Normality of titratable acidity measurements within each species was tested beforehand. In the
185 LMM model, titratable acid represents the dependent variable, while watering regime and time
186 point are fixed effects, and their interaction is included into the model. To control for random
187 variation in titratable acidity measurements across replicates of the same time point and watering
188 regime, the model includes a random intercept for each replicate. The analysis was performed
189 using the *lmer* function from R package *lme4* (Bates *et al.*, 2015). The goodness of fit of the model
190 was evaluated by plotting a QQ-Plot and the fitted values to residuals for each species. The
191 significance of fixed effects was evaluated by obtaining a p-value using the R package *lmerTest*
192 (Kuznetsova, Brockhoff and Christensen, 2017). A Tukey HSD test in the R package *emmeans*
193 was performed to assess the effects of individual watering regimes and time points on titratable
194 acidity.

195 To directly test for a difference between species in titratable acidity, we calculated the
196 maximum difference in titratable acidity (ΔTA) between day and night by subtracting the TA of
197 the two timepoints with the largest difference, which resulted to be TA_{N+10} - TA_{D+10} for all groups
198 (species and watering regime, see Fig. 2A). Significant differences in ΔTA for watering regime
199 and species were tested with ANOVA and Tukey HSD. We performed Shapiro-Wilk and Levene's

200 tests to ascertain that the assumptions of normality and homogeneity of variances were met. The
201 model used for ANOVA was ΔTA ~ species * watering regime.

202 **3.3. RNA extraction and sequencing**

203 RNA-seq data was obtained for samples at timepoints 10 am (D+4) and 10 pm (N+4) for
204 two watering regimes and two species (24 samples in total). Total RNA was extracted using the
205 QIAGEN RNeasy® Mini Kit. We evaluated the purity and concentration of the extractions using
206 Nanodrop, RIN and fragmentation profiles were obtained with a BioAnalyzer™ (Table S1). RNA
207 library preparation and poly-A capture were performed at the Vienna Biocenter Core Facilities
208 (VBCF) using a NEBNext stranded mRNA kit. The libraries were sequenced on one lane of
209 Illumina NovaSeq SP 150 PE flowcells.

210 **3.4. RNA-seq data processing**

211 Raw sequence quality was assessed using FastQC v. 0.11.8
212 (https://www.bioinformatics.babraham.ac.uk/projects/fastqc/) and MultiQC (Ewels *et al.*, 2016).
213 Adapters and low-quality bases were trimmed off using AdapterRemoval v. 2.3.1 (Schubert,
214 Lindgreen and Orlando, 2016) with settings --trimns --trimqualities --minquality 20 --
215 trimwindows 12 --minlength 36. The trimmed data was aligned to the *T. fasciculata* reference
216 genome (GenBank accession: GCA_029168755.2, Groot Crego et al. (2024) with STAR v. 2.7.3a
217 (Dobin *et al.*, 2013) in one pass using a GFF file to specify exonic regions.

218 **3.5. Differential gene expression analysis**

219 Read counts were quantified per exon for paired-end and reversely stranded reads (options
220 -p, -s 2) in the subread package FeatureCounts v. 2.0.2 (Liao, Smyth and Shi, 2014), after which
221 the counts of all exons of a gene were summed up to obtain per-gene counts. Differential gene
222 expression (DGE) analyses were performed for each species separately using the Bioconductor
223 package edgeR v. 3.40.0 (Robinson, McCarthy and Smyth, 2009).
224 We built a design matrix incorporating the two investigated treatments (timepoint and
225 watering regime). Genes where three or fewer samples of the same species had a Counts Per
226 Million (cpm) value smaller or equal to 1 were filtered out. Library size normalisation was done
227 using edgeR's default trimmed mean of M-values (TMM) normalisation method (Robinson and
228 Oshlack, 2010). The Cox-Reid profile-adjusted likelihood (CR) method was used to estimate

229 dispersion. Genes were tested for differential expression between timepoints and between watering
230 regimes separately for each species by fitting a negative binomial General Linear Model (GLM)
231 with the following contrasts: Day versus Night at control = Day_control - Night_control, Day
232 versus Night at drought = Day_drought - Night_drought, Drought vs Control at day = Drought_day
233 - Control_day, Drought vs Control at night = Drought_night - Control_night.
234 To test the fit of these GLM's, we conducted a quasi-likelihood F-test. The level of
235 significance was adjusted with the Benjamini-Hochberg correction method to account for multiple
236 testing. Genes were considered differentially expressed when the adjusted p-value was below 0.05
237 and the expression had an absolute log-fold change of at least 1.5. The total number of
238 differentially expressed genes for each treatment (timepoint and watering regime) was then
239 visualised and compared between species using ggplot2.

240 **3.6. Venn-diagrams**

241 To understand the extent of shared response to drought between both species, differentially
242 expressed genes were visualised with Venn diagrams using the R package VennDiagram (Chen
243 and Boutros, 2011). Diagrams were made for the overlap of differentially expressed (DE) genes
244 between watering regimes (control and drought) at different timepoints, and for the overlap in DE
245 genes between timepoints (day and night) at different watering regimes.
246 To test whether overlaps in DE genes between species, conditions and timepoints were
247 larger or smaller than expected by random sampling, we performed a hypergeometric test in the R
248 package SuperExactTest (Wang, Zhao and Zhang, 2015). Since separate DE analyses were
249 performed for each species, the starting set of filtered genes differed between species. However,
250 the size of the starting set of genes was highly comparable between the two species, with 17,899
251 filtered genes in *T. vanhyningii* and 17,676 in *T. leiboldiana*, of which 92.5 % overlap. We
252 therefore performed the hypergeometric test by taking the average filtered gene set size between
253 the two species, and obtaining p-values for every overlap present in the Venn-diagrams.

254 **3.7. Functional interpretation of DE genes**

255 Gene Ontology (GO) enrichment analyses were performed for both sets of DE genes (time
256 point and watering regime) within both species using the Bioconductor package topGO v. 2.50.0.
257 (Alexa, Rahnenführer and Lengauer, 2006). Significance of enrichment was evaluated with the

258 Fisher exact test and the algorithm "weight01". The top 100 significant GO terms were then
259 compiled sorted by decreasing significance using a custom-made script available at the repository
260 https://github.com/cgrootcrego/Tillandsia_CAM-Drought.

261 Aside from performing GO enrichment analyses on the full subset of DE genes, we also
262 performed enrichment analyses on each subset of genes representing a section in the Venn-
263 diagrams whenever it contained more than 25 genes, to functionally describe the overlap between
264 species and conditions.

265 Complementary to a GO enrichment analysis, we identified genes previously described as
266 related to CAM, starch metabolism and glycolysis in the same manner as described in Groot Crego
267 et al. 2024. Briefly, the extensive list of *A. comosus* gene ID's representing genes underlying
268 CAM, starch metabolism or glycolysis compiled by (2021) based on a diverse set of studies was
269 used to obtain the ID of *T. fasciculata* orthologous genes. This resulted in a total of 815 genes. The
270 genes from this subset that were differentially expressed in any of the comparisons were then
271 grouped by their overlap between species as indicated in the Venn diagrams.

272 The abundance of RNA reads for a select group of 74 CAM-related genes was plotted in a
273 heatmap using the R package ComplexHeatmap (Gu, Eils and Schlesner, 2016) for all 24 samples.
274 This subset includes 12 *T. fasciculata* orthologs of all pineapple genes putatively described as part
275 of the CAM carbon-fixation module (hereafter referred to as "Core CAM genes") (Ming *et al.*,
276 2015), regardless of their differential expression status. The remaining 62 genes include
277 aquaporins (5), circadian clock regulators (15), drought resistance genes (5), malate transporters
278 (2), photosystem-related genes (9), vacuolar proton pumps (13), genes related to stomatal
279 movement (7), vacuolar sugar invertases (3) and sugar transporters (3). Reads were normalised
280 with the TPM (Transcripts Per Million) method using total exonic length of each gene, and
281 converted to a log10 scale, then mean-centred with a z-score transformation. A separate heatmap
282 was made exclusively for homologs of the *PEPC* and *PPCK* genes.

283 **3.8. Gene trees of PPC1, PPC2 and PPCK**

284 We identified homologs of the two subfamilies of PEPC, PPC1, PPC2 and of PPCK by
285 running BLASTP on the available gene models of *A. comosus* (V3), *Sorghum bicolor* (v3.1.1),
286 *Oryza sativa* (v7.0), *Zea mays* (RefGen v.4), *Asparagus officinalis* (V1.1) and *Arabidopsis*
287 *thaliana* (TAIR10) on Phytozome (https://phytozome-next.jgi.doe.gov/), using the known

288 *Tillandsia* homologs of pineapple PEPC and PPCK genes (Groot Crego *et al.*, 2024). Hits were
289 filtered based on identity and target length for each respective gene. For PPC1, we selected all
290 targets longer than 500 aa and with more than 80% identity, resulting in 56 protein sequences
291 across the seven species. For PPC2, the identity threshold was lowered to 70 %, resulting in eight
292 sequences. For PPCK, we selected all sequences with an identity greater than 60 % regardless of
293 target length, resulting in 17 sequences.

294 Protein sequences were aligned using mafft v.7.520 (Katoh *et al.*, 2002) with options *--op*
295 *1.5 --ep 0.1 --maxiterate 1000 --localpair*. Gene trees were constructed using IQTREE v.2.2.5
296 (Minh *et al.*, 2020) with options *-B 1000 -T AUTO*. The resulting consensus tree was used for
297 visualisation, collapsing branches leading to Poaceae genes.

298

299 **4. Results**

300 **4.1. Titratable acidity measurements**

301 In control conditions, titratable acidity displays a CAM-like diel curve in *T. vanhyningii*,
302 with an overnight accumulation of acids and depletion throughout the day (Figure 2A, Table S2).
303 Our LMM model shows TA fluctuates significantly between timepoints both under control and
304 drought conditions, yet there is no significant difference in TA values between watering regimes
305 at the same time point (Fig. S1, Table S3). In *T. leiboldiana*, TA does not appear to accumulate
306 overnight in control conditions, as differences between time points in the LMM model are not
307 significant. Under drought conditions, TA values between D+10 and N+10 are significantly
308 different, indicating a slight fluctuation in leaf acidity. *T. leiboldiana* exhibits a markedly different
309 temporal curve in TA accumulation between control and drought conditions, as the difference in
310 TA values between watering regimes at each time point is significantly different in all but one time
311 point (Table S3)t.

312 The maximum difference in TA (ΔTA) reflects the degree of acid accumulation over time
313 and is significantly different between species (ANOVA p-value = 0.00406, Table S3) but not
314 between watering regimes (p-value = 0.473). Overall, our analysis of TA indicates that diel
315 metabolism in the two species is substantially different, and so is their response to drought. While
316 *T. vanhyningii*'s TA curve shows strong oscillation under control conditions, which is
317 characteristic for constitutive CAM, it appears nearly identical under drought except for an earlier
318 accumulation at N+4. *T. leiboldiana*'s TA curve shows no significant fluctuation under control

conditions, which is characteristic of a C3 plant, yet some diel fluctuation becomes apparent under drought, indicating a weak, facultative CAM cycle.

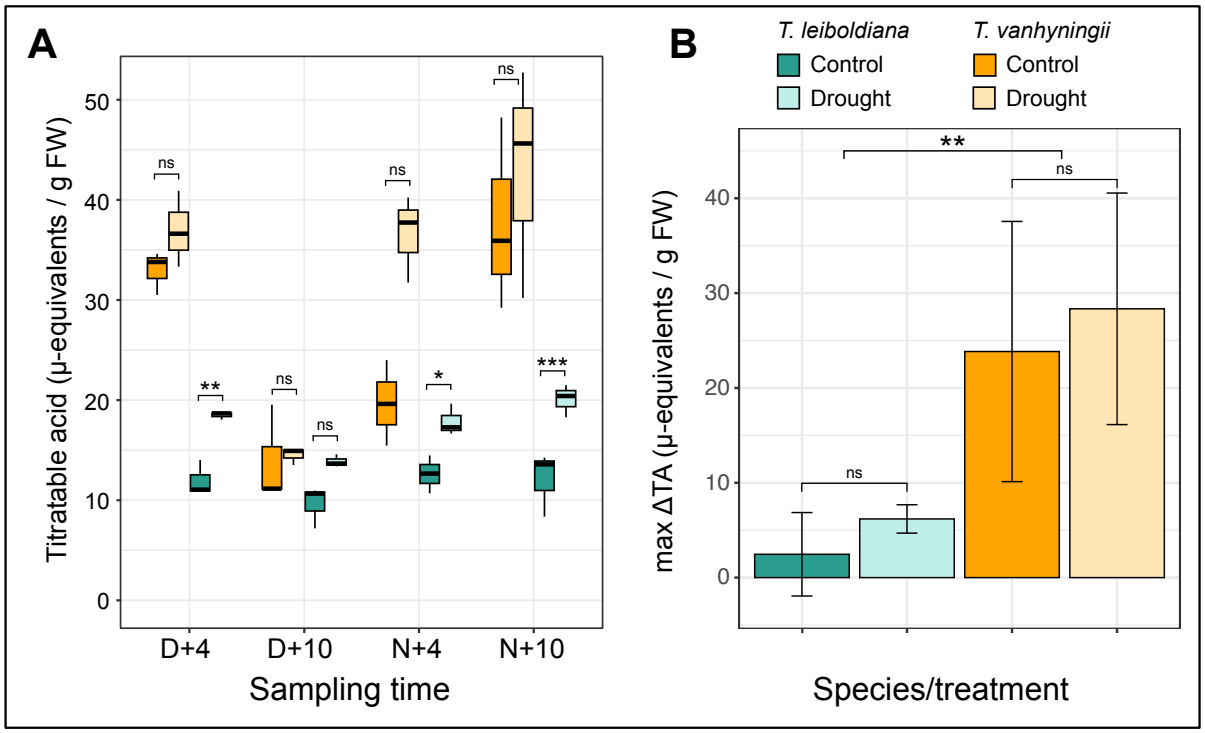

Figure 2: Titratable Acidity (TA) measurements of T. vanhyningii *and* T. leiboldiana*.* ***A)*** *Titratable acidity measured at four time points across a diel cycle under two watering regimes. The significance level of within-species, between-watering regime comparisons at a given time point from an LMM model are shown with following thresholds: ns - p-value > 0.05; * - p-value < 0.05; ** - p-value < 0.01; *** - p-value < 1E-03.* ***B)*** *Maximum difference in titratable acidity across a diel cycle for both species in two watering regimes. The bar plots represent the average ΔTA measured across replicates, error bars represent the standard deviation. The significance level from the ANOVA test is shown with the same thresholds as in A).*

4.2. Differential gene expression

Mapping to the *T. fasciculata* reference genome was highly uniform between species, with the median proportion of reads mapping uniquely being the same for *T. leiboldiana* and *T. vanhyningii* (Fig. S2). After assigning RNA-seq reads to genes, we obtain on average 49,266,700 ± 5,734,213 uniquely assigned reads per sample (Table S4). On average, 69 % ± 1 % of the full *T. fasciculata* annotated gene set had non-zero counts per individual. The variance in read counts per individual is largely explained by species-specific differences, as the first component of the PCA

separates samples clearly by species and explains 44.9 % of variance (Fig. S3), exceeding differences in gene expression between day and night, or between watering regimes. Therefore, DGE analyses were performed separately for each species.

DGE analyses reveal widely different counts of DE genes along the time and watering regime axes. In both species, many genes are DE between day and night, regardless of watering

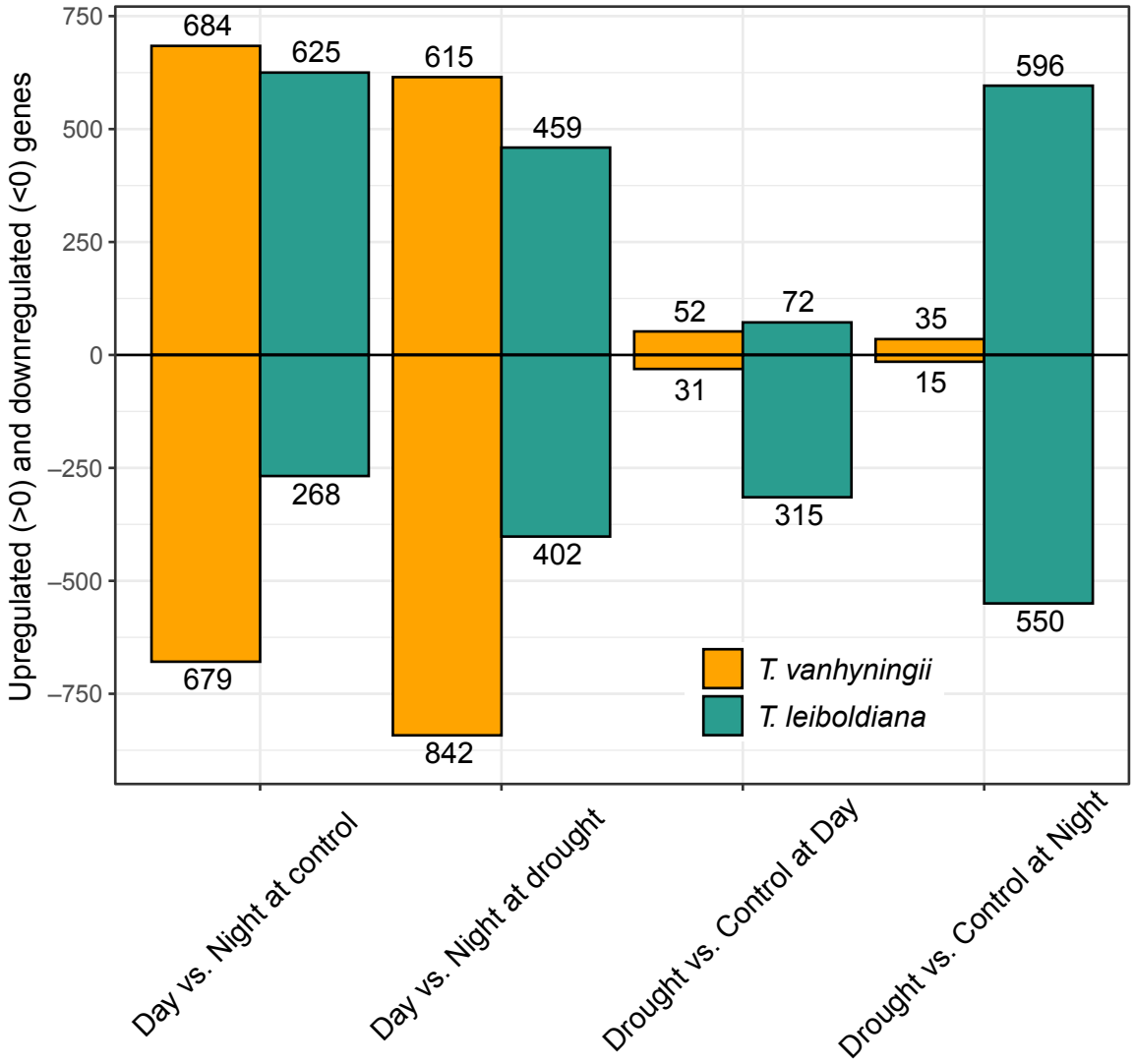

Figure 3: Counts of up- and down-regulated DE genes (adjusted p-value < 0.05, |FDR| ≥ 1.5) in four comparisons of different conditions: diel differences in two watering regimes (first four bars), and differences due to watering regimes at two timepoints (last four bars). The analyses were conducted in each species separately. Up-regulation reflects increased expression at day compared to night for timewise comparisons, and in drought compared to control conditions for comparisons of watering regimes.

347 regime (Fig. 3). However, *T. vanhyningii* consistently exhibits a closer resemblance in day-
348 versus-night activity compared to *T. leiboldiana*. The transcriptomic activity in *T. vanhyningii*
349 under control conditions is comparable between day and night, with only a 2.5 % increase in
350 upregulated genes at night than at day. In comparison, *T. leiboldiana* has 2.4x more genes
351 upregulated at day than at night in control conditions. This difference could reflect the more equal
352 task division between day and night in CAM plants compared to plants with a C3-like metabolism,
353 where most of the photosynthetic apparatus operates during the day. Under drought conditions,
354 transcriptomic activity shifts towards the night in both species. While this pattern is noticeable in
355 *T. vanhyningii*, with 58 % of DE genes upregulated at night under drought compared to 51 % in
356 control, it is especially pronounced in *T. leiboldiana*, where 47 % of genes is upregulated at night
357 under drought compared to 30 % in control.

358 In comparison with time-wise analyses, much fewer genes are DE between watering
359 regimes, except in *T. leiboldiana* at night. Here, *T. vanhyningii* appears to show a particularly
360 similar expression between the watering regimes independent on the time point, as opposed to *T.*
361 *leiboldiana*. DE gene counts are low for *T. vanhyningii* both at day and at night, suggesting that
362 most temporal expression patterns detected in the time-wise DGE analysis are constitutive.

363 Compared to *T. vanhyningii*, *T. leiboldiana* manifests a much more noticeable response to
364 drought, especially at night. During the day, transcriptomic activity seems decreased under
365 drought, as only 20 % of DE genes are upregulated. The total number of DE genes between
366 watering conditions at night is 2.8x larger than at day, which is a contrary trend to *T. vanhyningii*.

367 **4.3. Overlap in transcriptomic response**

368 The hypergeometric test revealed that all detected overlaps between species, time points
369 and watering regimes are larger than expected by random chance, indicating that the same
370 biological processes were captured between species and watering regimes by our RNA-seq
371 experiment (Table S5). The timewise transcriptomic response has a large overlap between species
372 and watering regimes, with 53 % of all DE genes being unique to one species and watering regime
373 (Fig. 4A). While this is to be expected given all plants experience day-night changes, only 5.9 %
374 of all timewise DE genes are shared between all groups. The largest overlap is found within species
375 between conditions, as only 19 % of all time-wise DE genes are shared between species (Table
376 S6). The overlap in timewise DE genes between watering regimes is greater in *T. vanhyningii* (44

377 %) than in *T. leiboldiana* (35 %). Conversely, the two species share more timewise DE genes
378 under drought conditions (17 %) than in control conditions (14 %).
379 In comparison, the response to watering regime is largely non-shared between groups, with
380 77 % of all DE genes being unique to one species and timepoint and only two DE genes being
381 shared among all groups (Fig. 4B). *T. vanhyningii* shows little overlap between time points in the
382 response to drought (8 %), while in *T. leiboldiana* 22 % of genes are DE between watering regimes
383 at both timepoints (Table S6). Due to the small number of DE genes in *T. vanhyningii* between
384 watering regimes, the overlap between species is negligibly small (2.4 %) in proportion to the
385 number of DE genes called in *T. leiboldiana*.
386 In summary, both the overall transcriptomic response to day-night changes and to watering
387 regimes shows little overlap between species, yet diel expression between species seems to overlap
388 slightly more under drought than under control, indicating an increase in the resemblance of the
389 two species' metabolism under drought stress.

390 **4.4. CAM-related transcriptomic overlap and differences between species,**
391 **timepoints and conditions**

392 **4.4.1. Overlap between species**

393 A CAM-related change in expression is likely to be associated both with differential
394 expression between time points as between watering regimes in *T. leiboldiana*, which seems to
395 activate a CAM cycle under drought conditions. When considering all DE genes summed up across
396 species, time points and watering regimes, 582 were DE in at least one of the two timewise DE
397 analyses across species and in at least one of the two watering-regime DE analyses. This number
398 represents 25 % of all genes with time-structured activity in at least one species, 43 % of all genes
399 that are DE between watering conditions in at least one species and 17 % of all DE genes
400 combined.
401 Of these 582 genes, the largest group is DE in *T. leiboldiana* for both time and watering
402 regime, but not DE in *T. vanhyningii* (Fig. 5). The second largest group consists of 151 genes (26
403 %) which display a time-structured activity in *T. vanhyningii* while being DE between watering
404 regimes in *T. leiboldiana*, and includes nine previously described CAM-related genes, among
405 which the sugar transporter SWEET14. 137 genes (24 %) show a time-structured expression in
406 both species but are only DE between watering conditions in *T. leiboldiana*. Among these genes

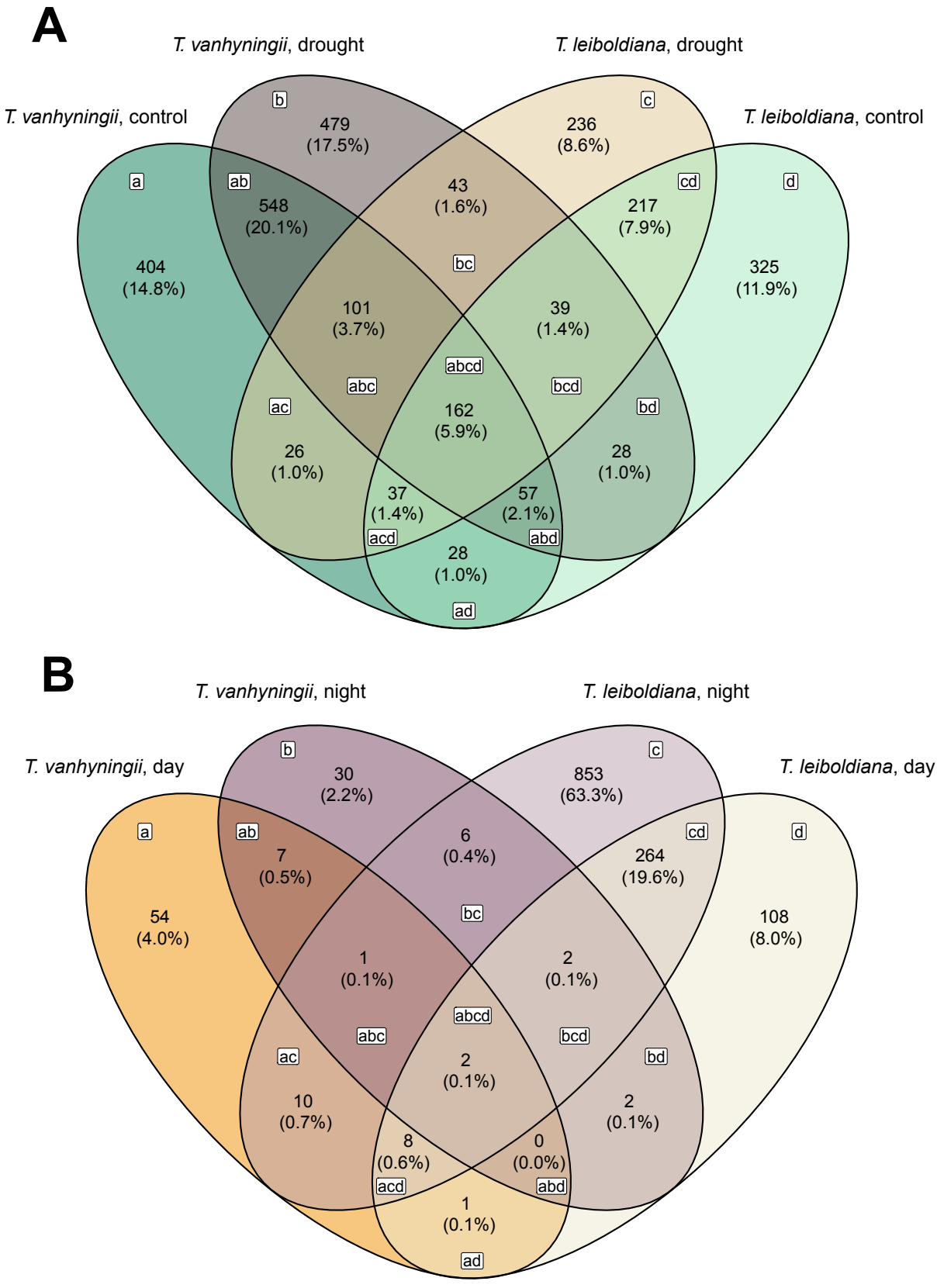
A
T. vanhyningii, drought
T. leiboldiana, drought
T. vanhyningii, control
T. leiboldiana, control
a
b
c
d
ab
ac
ad
bc
bd
cd
abc
abd
acd
bcd
abcd
404 (14.8%)
479 (17.5%)
236 (8.6%)
325 (11.9%)
548 (20.1%)
43 (1.6%)
217 (7.9%)
101 (3.7%)
39 (1.4%)
162 (5.9%)
26 (1.0%)
28 (1.0%)
37 (1.4%)
57 (2.1%)
28 (1.0%)
B
T. vanhyningii, night
T. leiboldiana, night
T. vanhyningii, day
T. leiboldiana, day
a
b
c
d
ab
ac
ad
bc
bd
cd
abc
abd
acd
bcd
abcd
54 (4.0%)
30 (2.2%)
853 (63.3%)
108 (8.0%)
7 (0.5%)
6 (0.4%)
264 (19.6%)
1 (0.1%)
2 (0.1%)
2 (0.1%)
10 (0.7%)
2 (0.1%)
8 (0.6%)
0 (0.0%)
1 (0.1%)

407

408 *Figure 4: Overlap of species-specific DE gene lists between timepoints and watering regimes.* ***A)*** *Venn*
409 *diagram showing the number and proportion of shared timewise DE genes (i.e., Day versus Night) per*
410 *combined group of species and watering condition.* ***B)*** *Venn diagram showing the number and proportion*
411 *of shared DE genes between watering regimes (i.e., Drought versus Control) per combined group of species*
412 *and time point. Letters inside sections show the overlap between the four groups.*

413 were 16 previously described CAM-related genes, yet only four were upregulated at drought in *T.*
414 *leiboldiana*, including core CAM gene encoding for PEPC kinase (*PPCK2*), a drought resistance
415 gene YLS9 (Müller *et al.*, 2017), and two genes encoding enzymes associated with glycolysis and
416 gluconeogenesis. This shows that the overlap of CAM-related response to drought between species
417 is limited mostly to core CAM genes.

418 We also searched for CAM-related genes among the larger set of DE genes called across
419 time and watering regime separately. The set of timewise DE genes contained 101 and 86 CAM-
420 related genes in *T. vanhyningii* and *T. leiboldiana* respectively, and reveal a myriad of underlying
421 functions such as circadian clock, glycolysis, stomatal movement, drought resistance, and water
422 and sugar transport (Table S7). Overlap between species and watering regimes of these genes
423 follows approximately the same trend as the full set of DE genes, with 49 % of genes being unique
424 to a given species and watering regime (Table S6). The twelve CAM-related genes that are
425 differentially expressed between time points in all groups are related to the circadian clock,
426 photosynthesis, and photosystem activity, which are expected to constitutively show diel
427 expression in plants. In *T. vanhyningii,* 45 % of CAM timewise DE genes are shared between
428 watering conditions. On the other hand, *T. leiboldiana* only shares 36 % of genes between watering
429 conditions, showing a clearer shift in photosynthetic metabolism when drought-stressed. The
430 proportion of timewise CAM DE genes shared between species is similar in both watering regimes
431 (21 % at control and 22 % at drought), which is slightly higher than across all DE genes, but
432 remains a minority of the total set of CAM-related DE genes.

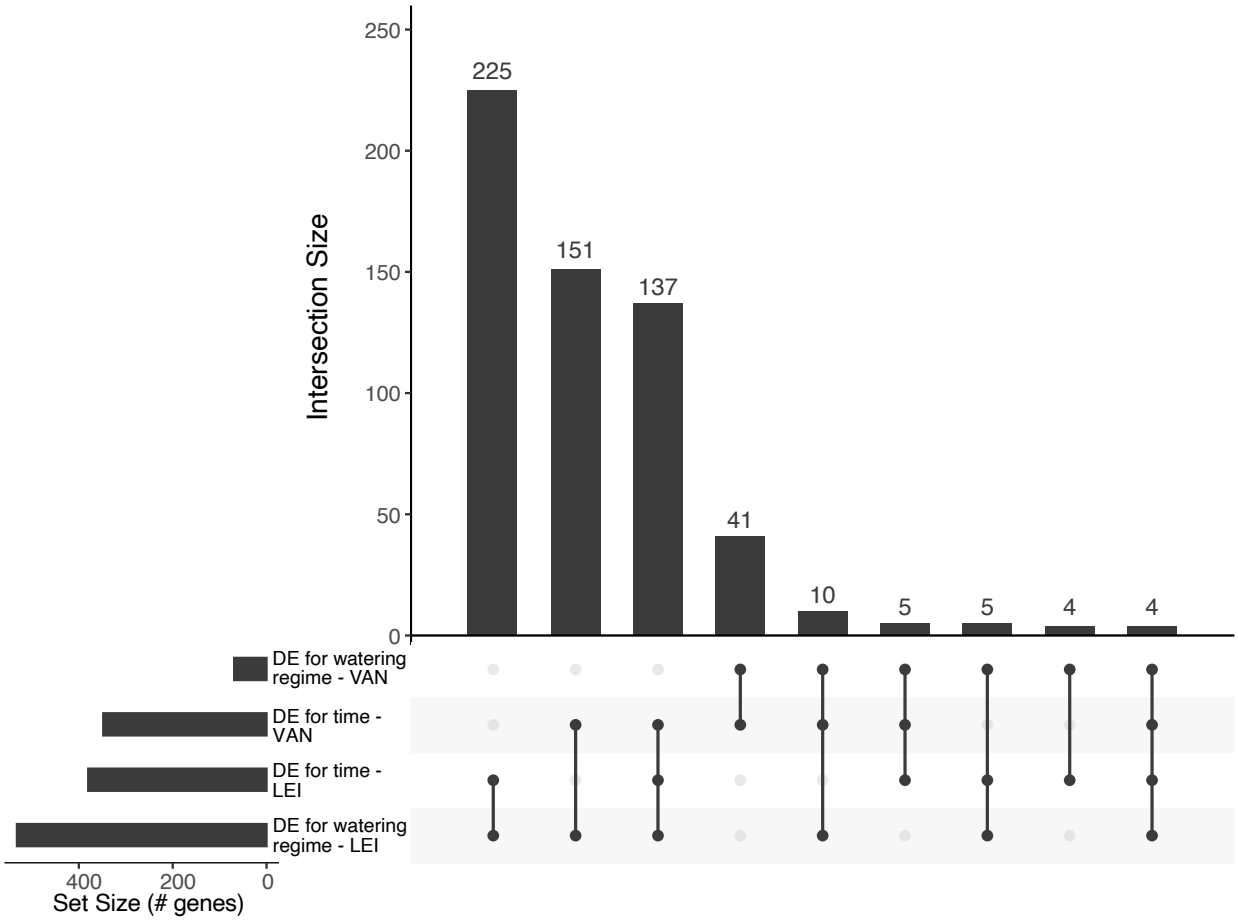

Figure 5: Overview of the overlap between DE analyses across time points and across watering regimes. The bar plots represent the number of genes overlapping between DE analyses, sorted in descending order. Below, the linked dots represent the analyses which display each overlap. The vertically oriented bar plot on the left-side shows the total number of DE genes called in each analysis. DE analyses were performed between time points and watering regimes in each species (VAN = T. vanhyningii*, LEI =* T. leiboldiana*)*

For DE genes between watering regimes, seven and 78 CAM-related genes were present in *T. vanhyningii* and *T. leiboldiana* respectively (Table S6, Table S8). In *T. vanhyningii*, only one gene was shared between timepoints, whereas in *T. leiboldiana* 28 % overlapped between timepoints. Only one gene overlapped between the species, namely a gene encoding for a probable linoleate 9S-lipoxygenase enzyme, which was found differentially expressed between C3 and CAM *Tillandsia* species in a previous study (De La Harpe *et al.*, 2020). Lipoxygenases are involved in the biosynthesis of jasmonates, which play an important role in response to various biotic and abiotic stressors (Bachmann *et al.*, 2002).

447 #### 4.4.2. CAM-related expression in *Tillandsia vanhyningii*

448 In control conditions, *T. vanhyningii* shows timewise differential expression of core CAM
449 gene PPCK and of genes underlying CAM-related functions such as stomatal movement, vacuolar
450 proton pumps, malate transport, sugar transport and glycolysis (Table S7). Several genes encoding
451 for Late Embryogenesis Abundant (LEA) proteins , which are linked to drought tolerance, also
452 show diel expression in control conditions, for example.

453 The set of CAM-related functions showing diel expression in drought conditions is similar
454 to that of control conditions and has an overlap of 46 genes, including PPCK, circadian clock
455 regulator REVEILLE1, a beta-amylase (starch breakdown), and all LEA proteins that are DE in
456 control. AVP1, a secondary proton pump that aids in the vacuolar transport of malate, is only DE
457 in control conditions, whereas a malate dehydrogenase is exclusively showing diel expression in
458 drought conditions. While sugar transporter SWEET16 shows diel expression exclusively under
459 control conditions, SWEET14 is exclusively DE in drought conditions. An additional set of LEA
460 proteins also become timewise DE in drought conditions. These findings suggest that, while the
461 CAM pathway of *T. vanhyningii* remains largely similar regardless of watering conditions,
462 different genes underlying the same functions are being co-opted under specific circumstances.

463 Very few CAM-related genes were DE in *T. vanhyningii* between watering regimes. They
464 include an aquaporin PIP2-4 (water transport) and several enzymes associated with glycolysis and
465 gluconeogenesis. None of these genes are part of the core CAM pathway, further showing the lack
466 of response to drought in the constitutive CAM species regarding its photosynthetic metabolism.

467 #### 4.4.3. CAM-related expression in *Tillandsia leiboldiana*

468 In *T. leiboldiana* at control conditions, identified CAM-related DE genes underlie functions
469 that are typically also expected to fluctuate across time in C3 plants (glycolysis and
470 gluconeogenesis, sugar transport, circadian clock regulation). Beta-carbonic anhydrase 2 is
471 timewise DE in control conditions, but is upregulated during the day (Fig. S4), which is contrary
472 to the expected nighttime activity in CAM. Under drought conditions, 31 DE genes overlap with
473 control conditions (Table S7), yet many additional CAM-related functions become timewise DE
474 under drought conditions, such as malate transport, stomatal movement, sugar metabolism, water
475 transport and starch metabolism. Genes encoding Alpha-carbonic anhydrase 1 (*α-CA*) and
476 phosphoenolpyruvate carboxylase kinase (*PPCK2*) are upregulated at night, along with circadian
477 clock regulator XAP5 CIRCADIAN TIMEKEEPER (XCT), which has been detected as

478 differentially expressed between CAM and C3-like *Tillandsia* in several studies (De La Harpe *et*
479 *al.*, 2020; Groot Crego *et al.*, 2024). These findings further emphasise that a CAM cycle is likely
480 activated in *T. leiboldiana* under drought conditions.

481 The comparison of gene expression between watering regimes at a given time point
482 confirms this finding even further. Most CAM-related genes that are DE between watering regimes
483 can be found in *T. leiboldiana* at night, and include the core CAM genes phosphoenolpyruvate
484 carboxylase (*PEPC*) and *PPCK* (Table S8).

485 **4.4.4. Diel expression of PPC and PPCK homologs between species and**
486 **watering regimes**

487 The transcript abundances of PEPC and PPCK homologs reveal a variety of expression
488 patterns. Gene *Tfasc_v1.16311-RA*, which is the ortholog of *PPC1-M1* (Fig. S5A) and was
489 previously identified as the CAM-related fluctuating copy of PEPC in *T. fasciculata* (Groot Crego
490 *et al.*, 2024) does not show clear diel expression changes in *T. vanhyningii* (Fig. 6). In *T.*
491 *leiboldiana* a slight increase is noticeable at night but it is not significant in either condition.
492 This could be explained by the time of sampling not being synchronous with the peaking and
493 troughing times of PEPC, and aligns with other core CAM enzymes not being timewise DE in this
494 experiment (Fig. S3). However, the enzyme is noticeably more highly expressed in *T. vanhyningii*
495 compared to *T. leiboldiana*. The remaining known *PEPC* genes are generally less expressed than
496 *PPC1-M1* in both species, but appear to become activated under drought conditions, namely in *T.*
497 *vanhyningii* for *PPC1-M2* (not significant), and in *T. leiboldiana* for *PPC2*.

498 For PEPC kinase (PPCK), diel expression stands out in one gene (*PPCK2,* Fig. S6) in *T.*
499 *vanhyningii* under both watering regimes. While not strongly expressed at night in control
500 conditions in *T. leiboldiana*, the gene copy becomes highly expressed under drought conditions,
501 which is perhaps the most direct indication of an activated CAM cycle in *T. leiboldiana* under
502 drought. *PPCK1* shows mild diel fluctuation in *T. vanhyningii* but is overall lowly expressed in *T.*
503 *leiboldiana*.

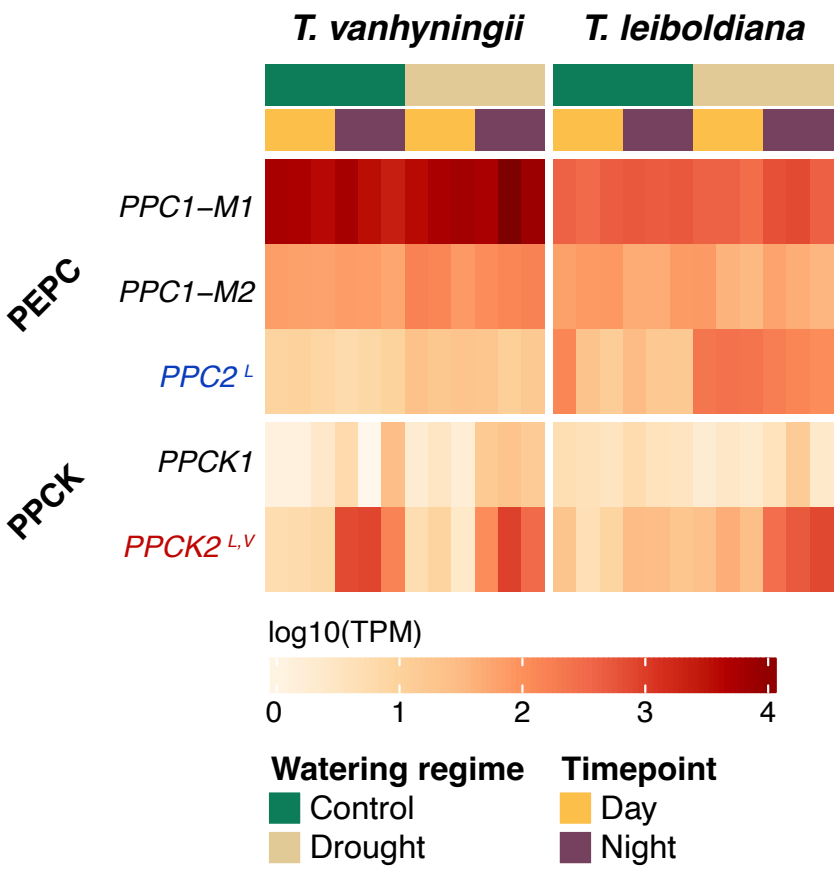

Figure 6: Transcript abundance in "Transcripts per Million" (TPM) for all homologous genes encoding for PEPC and PEPC kinase (PPCK) in T. vanhyningii *(left panel) and* T. leiboldiana *(right panel) at two timepoints and watering regimes. TPM values are transformed to a logarithmic scale. The colour of gene names reflects their differential expression status: blue = DE in Drought vs Control comparisons, red is DE in both comparisons and black = not DE. If a gene is DE, the species initial in which it was detected is mentioned in superscript behind its name.*

4.5. Description of the general response to drought

As described above, the quantitative response to drought is far greater in *T. leiboldiana* than in *T. vanhyningii* (Fig. 3), suggesting suggests that *T. leiboldiana*'s metabolism is being severely affected by drought, while *T. vanhyningii*'s seems largely the same between conditions. This demonstrates inherently the drought-tolerant nature of a constitutive CAM plant and contrasts it to the marked stress-response of a closely related weak CAM plant.

GO term enrichment of gene sets that are DE in *T. leiboldiana* between watering regimes further point at a drought response underlying the large-scale expression changes observed in this

species (Fig. 7A), with genes involved in the response to water deprivation and to the stress-hormone abscisic acid showing the strongest overall up-regulation at drought of all DE genes. Processes that are strongly under-regulated during drought reveal a general shutdown of metabolism, such as photosynthesis, transport, and biosynthetic processes.

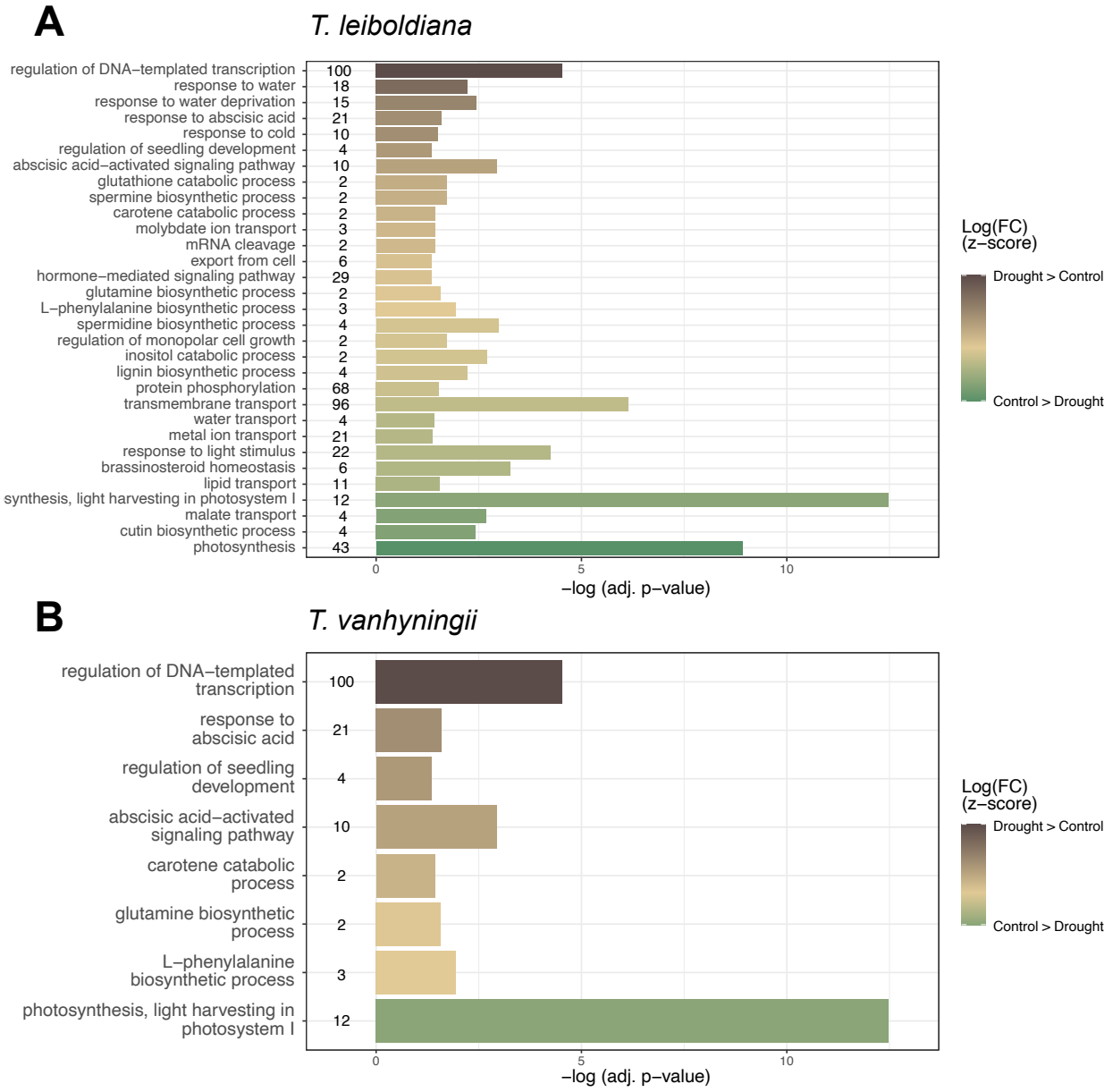

Figure 7: Summary of significantly enriched GO terms representing a Biological Process (BP) in DE genes between watering regimes in T. leiboldiana *(**A**) and* T. vanhyningii *(**B**). GO term enrichment at day and night were combined for each bar plot. The bars show the significance of each enriched GO term as the p-value adjusted for multiple-testing, on a logarithmic scale. The colour gradient shows the degree of overall up- and down-regulation of the genes underlying each GO term, as a z-score of the fold-change on a*

529 *logarithmic scale. The GO terms are shown in descending order from most up-regulated in drought*
530 *conditions to most up-regulated in control conditions.*

531 This contrasts strongly with enriched GO terms found among the few DE genes in *T.*
532 *vanhyningii*, where a response to drought is not immediately apparent - photosynthesis does not
533 seem to be regulated differently between watering regimes and no orchestrated response to water
534 deprivation is apparent (Fig. 7B). However, a few enriched GO terms do suggest a limited response
535 to drought, such as metabolism of inositol, jasmonate and molybdate.
536

537 **5. Discussion**

538 Crassulacean Acid Metabolism is associated with diversification in many plant families,
539 and described as a key innovation trait in Bromeliaceae (Benzing, 2000; Ogburn and Edwards,
540 2009; Silvera *et al.*, 2009; Quezada and Gianoli, 2011), yet the genetic architecture of the trait
541 itself, its degree of redundancy and genetic overlap between different forms, and its evolutionary
542 trajectory are not well understood (Edwards, 2023). The subgenus *Tillandsia* exhibits a broad
543 range of CAM phenotypes reflected in carbon isotope values (Crayn *et al.*, 2015; De La Harpe *et*
544 *al.*, 2020) and is an excellent system for studying CAM evolution, but the exact range of
545 phenotypes within the subgenus has not been characterised beyond carbon isotope ratios and
546 transcriptomic studies under control conditions. In this study, we compared physiological and
547 transcriptomic responses to drought between two species with some of the most extreme reported
548 carbon isotope ratios within the subgenus to further characterise the phenotypic range in the group
549 and elucidate the degree of shared transcriptomic response underlying two different CAM
550 phenotypes and their response to drought.

551 ***Tillandsia leiboldiana* is a weak CAM plant**

552 Both our time-wise titratable acidity measurements and differential gene expression
553 analysis indicate the presence of a latent CAM cycle in *T. leiboldiana* which becomes activated
554 under severe drought stress. The most direct evidence for this can be found in the nighttime
555 activation of *PPCK2* in *T. leiboldiana* in drought conditions, while it does not significantly
556 fluctuate over time in control conditions. Reported carbon isotope ratios for *T. leiboldiana* are well
557 within the C3 range ($\delta^{13}C$ = -28.0 / -31.3; Caryn et al. (2015), De La Harpe et al. (2020)), indicating
558 yet again the importance of characterising photosynthetic phenotypes at the hand of multiple

559 measurements performed in various environmental and developmental conditions. Instead of being
560 a strong C3 plant as the reported carbon isotope ratios suggest, *T. leiboldiana* is much more likely
561 to be a weak, facultative CAM plant performing C3 photosynthesis in optimal conditions but with
562 pre-existing CAM-like expression patterns in certain genes (Groot Crego *et al.*, 2024) and a weak
563 overnight accumulation of malate under drought conditions.

564 Due to a lack of gas exchange measurements, we can't yet establish whether *T. leiboldiana*
565 performs CAM cycling, i.e. malate production and storage starting from CO_2 accumulated during
566 the day, or instead, assimilates CO_2 overnight. The presence of several genes associated with
567 stomatal function among differentially expressed genes between watering regimes in *T.*
568 *leiboldiana* suggests a change in stomatal behaviour at drought conditions. However, this could be
569 a general response to drought rather than a CAM-specific response. For example, TRAB1, a
570 member of the abscisic acid signalling pathway, which is generally activated under drought stress
571 (Hobo, Kowyama and Hattori, 1999; Zhu, 2002), is upregulated in *T. leiboldiana* under drought
572 conditions at night (Fig. S4). On the other hand, the guard cell anion channel SLAC1, which
573 controls stomatal closure (Vahisalu *et al.*, 2008), is down-regulated at night in *T. leiboldiana* under
574 drought (Fig. S4), a potential indication that stomata open at night. Nonetheless, gas exchange
575 measurements are needed to fully understand stomatal activity and timing of CO_2 absorption in *T.*
576 *leiboldiana*.

577 **Response to drought is minimal in *Tillandsia vanhyningii***

578 Our physiological and transcriptomic analyses indicate very limited functional changes in
579 *T. vanhyningii* under drought conditions, especially compared to *T. leiboldiana*. Titratable acidity
580 is accumulated in a very similar manner among watering regimes, with the exception that
581 accumulation appears to occur faster overnight under drought conditions. This agrees with
582 previous studies on sister species *T. ionantha*, which showed that its physiology was little affected
583 even after six months of drought, and attributed its ability to maintain leaf water levels to day-time
584 closing of stomata, low stomatal densities and its enhanced ability to absorb water from the
585 atmosphere thanks to a dense layer of absorptive trichomes, (Nowak and Martin, 1997; Ohrui *et*
586 *al.*, 2007).

587 A very small number of genes were found to be DE between watering regimes in *T.*
588 *vanhyningii*, while a major response was detected in *T. leiboldiana*. Upregulated enriched GO

589 terms at drought in *T. vanhyningii* included metabolism of inositol, jasmonate, molybdate and
590 proline, all compounds known to play a role in drought response (Loewus and Murthy, 2000; Kim
591 *et al.*, 2004; Wasternack, 2014). This indicates that while *T. vanhyningii* shows minor signs of
592 response to drought, it is able to maintain most of its metabolism stable under drought stress, which
593 is not the case for *T. leiboldiana*.

594 These findings further support the view that "atmospheric" or "grey" *Tillandsia* such as *T.*
595 *vanhyningii* are drought-adapted, which has been shown in physiological studies (Martin, 1994;
596 Stiles and Martin, 1996; Nowak *et al.*, 1997; Castillo, Cervera and Navarro-Alberto, 2016), but to
597 our knowledge not on a broad transcriptomic or genomic level. Atmospheric *Tillandsia* represent
598 the most extreme forms of adaptation to an epiphytic lifestyle among Bromeliaceae, having lost
599 almost entirely the ability to absorb water with roots (Benzing, 2000; Crayn, Winter and Smith,
600 2004). They occur in arid habitats and are all constitutive CAM plants, leading to the suggestion
601 that CAM is a key innovation trait in this group (Crayn, Winter and Smith, 2004). Our findings
602 show indeed that *T. vanhyningii* is only mildly affected by drought conditions and points at
603 constitutive drought tolerance on the transcriptomic and physiological level in atmospheric
604 *Tillandsia*.

605 **Both response to drought and photosynthetic metabolism show little overlap between**
606 **species on the transcriptomic level**

607 *T. vanhyningii* and *T. leiboldiana* are closely related members of a recent radiation with an
608 estimated maximum divergence time of 3.22 Mya (Barfuss *et al.*, 2016; Mendoza *et al.*, 2017;
609 Yardeni *et al.*, 2023). Despite the relatively short time in which these species have diverged, our
610 analyses demonstrate clear differentiation on the physiological and transcriptomic level, resulting
611 in distinct photosynthetic phenotypes. On the transcriptomic level, both the set of time-structured
612 genes and the set of genes that are DE between watering regimes show little overlap between
613 species, which has also been reported in other CAM lineages such as Agavoideae (Heyduk,
614 McAssey and Leebens-Mack, 2022).

615 The majority of time-structured genes previously described as CAM-related are uniquely
616 time-structured within one species. This suggests that, despite *T. leiboldiana* appearing to activate
617 CAM under drought conditions, different sets of genes underlie this phenotype compared to *T.*
618 *vanhyningii*. A few notable exceptions of CAM-related genes that are shared between *T.*

619 *vanhyningii* and drought-stressed *T. leiboldiana* are *PPCK2* (Fig. 6), tonoplast dicarboxylate
620 transporter (malate transport) and protein YLS9 (drought resistance). The minor overlap in the
621 facultatively activated CAM cycle of *T. leiboldiana* and the constitutive cycle of *T. vanhyningii*
622 suggests a strong distinction in the transcriptomic basis leading to the two forms of CAM, rather
623 than a shared pathway which is expressed at lower levels in the weak CAM plant.

624 This is even more strongly supported by the distinct expression patterns of different gene
625 family members of PEPC. Under drought conditions, the homologous copy of *PPC2* appears to be
626 up-regulated in *T. leiboldiana*, while being lowly expressed at all conditions in *T. vanhyningii*.
627 Because none of the PEPC copies are time-structured in this experiment in any species or
628 condition, likely due to the time of sampling not being synchronous with the peak activity times
629 of this enzyme, it is difficult to confirm that *PPC2* is assimilated in CAM in *T. leiboldiana* under
630 drought conditions. While in the majority of CAM plant lineages, including *T. fasciculata* (Groot
631 Crego *et al.*, 2024) and *A. comosus* (Ming *et al.*, 2015), the PEPC gene copy recruited into the
632 CAM pathway is *PPC1*, recruitment of *PPC2* has been suggested in *Yucca aloifolia* (Heyduk,
633 McAssey and Leebens-Mack, 2022) and in *Isoetes taiwanensis* (Wickell *et al.*, 2021).

634 **Conclusion**

635 Taken together, this study characterises in detail the photosynthetic phenotypes of two
636 species of the subgenus *Tillandsia*, and illustrates that the species with one of the most C3-like
637 carbon isotope value recorded in the group so far is not a C3 plant, but a weak CAM intermediate.
638 While our findings suggest that the subgenus *Tillandsia* likely doesn't contain candidate C3
639 species, and therefore doesn't cover the full range of existing phenotypes in the C3-CAM
640 continuum known from other plant groups, our analyses also demonstrate an important distinction
641 on the transcriptomic level between weak and constitutive CAM. While on the phenotypic level,
642 both plants exhibit a similar phenotype at different rates, we find little overlap in the underlying
643 transcriptomic response. This highlights the polygenic nature of CAM and provides a hypothesis
644 for the high rate at which this trait has evolved independently across the plant kingdom; namely
645 the presence of multiple genetic routes to achieve similar phenotypes. Our findings also put in
646 question the idea of CAM being a trait with a single transcriptomic basis expressed to different
647 degrees in the phenotypic continuum between weak and strong CAM phenotypes. There is still a
648 broad diversity of intermediate CAM phenotypes and genotypes to be characterised in further

649 detail, and the subgenus *Tillandsia* with its wide range of intermediate CAM species forms an
650 excellent candidate group for future exciting research into the CAM continuum and its evolution.
651

652 **6. Acknowledgements**

653 This work was financially supported by the Austrian Science Fund (FWF) with grant
654 https://doi.org/10.55776/W1225 to a faculty team including C.L. and O.P., and grant
655 https://doi.org/10.55776/P35275 to O.P. Additionally, this work was funded by the professorship
656 start-up grant of Christian Lexer at the University of Vienna BE772002. We thank Viktor Vagovic
657 at the Core Facility Botanical Garden of the University of Vienna for caretaking and maintenance
658 of the plant accessions used in this study and assistance with the drought experiment. We also
659 thank Aglaia Szukala, Marta Pelizzola, Nina Flowers and Simon Reynaert for advice and
660 discussion on transcriptome analysis.
661

662 **7. Competing interests**

663 The authors declare no conflict of interests.
664

665 **8. Author Contributions**

666 This study was conceived by CL, JH, MDH, OP, and CGC. The greenhouse experiment and
667 sampling was conducted by MDH and MHJB. Laboratory work including titratable acidity
668 measurements and DNA extraction and library prep was conducted by MDH, OP and MHJB.
669 Analyses were performed by CGC, MDH and SS. The manuscript was primarily written by CGC
670 with contributions from SS, and amended following the dedicated reading and feedback of all co-
671 authors.
672

673 **9. Data availability**

674 Titratable acidity measurements, detailed information on statistical testing and accession
675 information is provided in the supplementary tables of this manuscript. The raw RNA-seq reads
676 will be deposited on the NCBI SRA database upon publication of this manuscript. Scripts, read
677 counts and extended tables of GO term enrichment analyses will be made available on the
678 following repository: https://github.com/cgrootcrego/Tillandsia_CAM-Drought.
679

10. References

Alexa, A., Rahnenführer, J. and Lengauer, T. (2006) "Improved scoring of functional groups from gene expression data by decorrelating GO graph structure," *Bioinformatics* , 22(13), pp. 1600–1607.

Bachmann, A. *et al.* (2002) "Jasmonate-induced lipid peroxidation in barley leaves initiated by distinct 13-LOX forms of chloroplasts," *Biological chemistry*, 383(10), pp. 1645–1657.

Barfuss, M. H. J. *et al.* (2016) "Taxonomic revision of bromeliaceae subfam. Tillandsioideae based on a multi-locus DNA sequence phylogeny and morphology," *Phytotaxa*, 279(1), pp. 1–97.

Barghi, N. *et al.* (2019) "Genetic redundancy fuels polygenic adaptation in Drosophila," *PLoS biology*, 17(2), p. e3000128.

Barghi, N., Hermisson, J. and Schlötterer, C. (2020) "Polygenic adaptation: a unifying framework to understand positive selection," *Nature reviews. Genetics*, 21(12), pp. 769–781.

Bates, D. *et al.* (2015) "Fitting Linear Mixed-Effects Models Using lme4," *Journal of statistical software*, 67, pp. 1–48.

Benzing, D. H. (2000) *Bromeliaceae: Profile of an Adaptive Radiation*. Cambridge University Press.

Beutelspacher, C. R. and García-Martínez, R. (2021) "Descripción de nuevos híbridos y una nueva combinación en Tillandsia (Bromeliaceae) para Chiapas, México," *Lacandonia*, 15(2), pp. 19–28.

Borland, A. M. *et al.* (2014) "Engineering crassulacean acid metabolism to improve water-use efficiency," *Trends in plant science*, 19(5), pp. 327–338.

Castillo, R. J., Cervera, J. C. and Navarro-Alberto, J. (2016) "Drought and extreme temperature tolerance for Tillandsia dasyliriifolia, an epiphytic bromeliad from the northern coastal dune scrubland in Yucatan, Mexico," *Botanical Sciences*, 94(1), pp. 121–126.

Chen, H. and Boutros, P. C. (2011) "VennDiagram: a package for the generation of highly-customizable Venn and Euler diagrams in R," *BMC bioinformatics*. bmcbioinformatics.biomedcentral …, 12, p. 35.

Crayn, D. M. *et al.* (2015) "Photosynthetic pathways in Bromeliaceae: Phylogenetic and ecological significance of CAM and C3 based on carbon isotope ratios for 1893 species," *Botanical journal of the Linnean Society. Linnean Society of London*. Blackwell Publishing Ltd, 178(2), pp. 169–221.

Crayn, D. M., Winter, K. and Smith, J. A. C. (2004) "Multiple origins of crassulacean acid metabolism and the epiphytic habit in the Neotropical family Bromeliaceae," *Proceedings of the National Academy of Sciences*. National Academy of Sciences, 101(10), pp. 3703–3708.

De La Harpe, M. *et al.* (2020) "Genomic footprints of repeated evolution of CAM photosynthesis in a Neotropical species radiation," *Plant, cell & environment*, 43(12), pp. 2987–3001.

Dobin, A. *et al.* (2013) "STAR: Ultrafast universal RNA-seq aligner," *Bioinformatics* . Oxford Academic, 29(1), pp. 15–21.

Edwards, E. J. (2023) "Reconciling continuous and discrete models of C4 and CAM evolution," *Annals of botany*. doi: 10.1093/aob/mcad125.

Ewels, P. *et al.* (2016) "MultiQC: summarize analysis results for multiple tools and samples in a single report," *Bioinformatics* , 32(19), pp. 3047–3048.

Gibson, A. C. (1982) "The anatomy of succulence," *Crassulacean acid metabolism*. American Society of Plant Physiologists Rockville, MD, USA, pp. 1–17.

Gilman, I. S. *et al.* (2023) "The CAM lineages of planet Earth," *Annals of botany*, 132(4), pp. 627–654.

Givnish, T. J. *et al.* (2014) "Adaptive radiation, correlated and contingent evolution, and net species diversification in Bromeliaceae," *Molecular phylogenetics and evolution*. Academic Press, 71(1), pp. 55–78.

Goldstein, D. B. and Holsinger, K. E. (1992) "Maintenance of polygenic variation in spatially structured populations: roles for local mating and genetic redundancy," *Evolution; international journal of organic evolution*, 46(2), pp. 412–429.

Griffiths, H. *et al.* (2008) "Leaf succulence determines the interplay between carboxylase systems and light use during Crassulacean acid metabolism in Kalanchoë species*," *Journal of experimental botany*. Oxford Academic, 59(7), pp. 1851–1861.

Groot Crego, C. *et al.* (2024) "CAM evolution is associated with gene family expansion in an explosive bromeliad radiation," *The Plant cell*. doi: 10.1093/plcell/koae130.

Gu, Z., Eils, R. and Schlesner, M. (2016) "Complex heatmaps reveal patterns and correlations in multidimensional genomic data," *Bioinformatics* , 32(18), pp. 2847–2849.

Hämälä, T. *et al.* (2020) "Gene Expression Modularity Reveals Footprints of Polygenic Adaptation in Theobroma cacao," *Molecular biology and evolution*, 37(1), pp. 110–123.

Heyduk, K. *et al.* (2016) "Gas exchange and leaf anatomy of a C3-CAM hybrid, Yucca gloriosa (Asparagaceae)," *Journal of experimental botany*, 67(5), pp. 1369–1379.

Heyduk, K. *et al.* (2018) "Shifts in gene expression profiles are associated with weak and strong Crassulacean acid metabolism," *American journal of botany*, 105(3), pp. 587–601.

Heyduk, K., McAssey, E. V. and Leebens-Mack, J. (2022) "Differential timing of gene expression and recruitment in independent origins of CAM in the Agavoideae (Asparagaceae),"

The New phytologist, 235(5), pp. 2111–2126.

Heyduk, K., Ray, J. N. and Leebens-Mack, J. (2021) "Leaf anatomy is not correlated to CAM function in a C3+CAM hybrid species, Yucca gloriosa," *Annals of botany*, 127(4), pp. 437–449.

Hobo, T., Kowyama, Y. and Hattori, T. (1999) "A bZIP factor, TRAB1, interacts with VP1 and mediates abscisic acid-induced transcription," *Proceedings of the National Academy of Sciences of the United States of America*, 96(26), pp. 15348–15353.

Katoh, K. *et al.* (2002) "MAFFT: a novel method for rapid multiple sequence alignment based on fast Fourier transform," *Nucleic acids research*, 30(14), pp. 3059–3066.

Kim, T.-H. *et al.* (2004) "De novo protein synthesis in relation to ammonia and proline accumulation in water stressed white clover," *Functional plant biology: FPB*, 31(8), pp. 847–855.

Kuznetsova, A., Brockhoff, P. B. and Christensen, R. H. B. (2017) "lmerTest Package: Tests in Linear Mixed Effects Models," *Journal of statistical software*, 82, pp. 1–26.

Láruson, Á. J., Yeaman, S. and Lotterhos, K. E. (2020) "The Importance of Genetic Redundancy in Evolution," *Trends in ecology & evolution*, 35(9), pp. 809–822.

Liao, Y., Smyth, G. K. and Shi, W. (2014) "FeatureCounts: An efficient general purpose program for assigning sequence reads to genomic features," *Bioinformatics* . Oxford University Press, 30(7), pp. 923–930.

Loewus, F. A. and Murthy, P. P. N. (2000) "myo-Inositol metabolism in plants," *Plant science: an international journal of experimental plant biology*, 150(1), pp. 1–19.

Males, J. (2018) "Concerted anatomical change associated with crassulacean acid metabolism in the Bromeliaceae," *Functional plant biology: FPB*, 45(7), pp. 681–695.

Martin, C. E. (1994) "Physiological ecology of the Bromeliaceae," *The Botanical review; interpreting botanical progress*, 60(1), pp. 1–82.

Martin, C. E., Hsu, R. C.-C. and Lin, T.-C. (2009) "The relationship between CAM and leaf succulence in two epiphytic vines, Hoya carnosa and Dischidia formosana (Asclepiadaceae), in a subtropical rainforest in northeastern Taiwan," *Photosynthetica*, 47(3), pp. 445–450.

Mendoza, C. G. *et al.* (2017) "Geographic structure in two highly diverse lineages of Tillandsia (Bromeliaceae)," *Botany*, 95(7), pp. 641–651.

Ming, R. *et al.* (2015) "The pineapple genome and the evolution of CAM photosynthesis," *Nature genetics*. Nature Publishing Group, 47(12), pp. 1435–1442.

Minh, B. Q. *et al.* (2020) "IQ-TREE 2: New Models and Efficient Methods for Phylogenetic Inference in the Genomic Era," *Molecular biology and evolution*, 37(5), pp. 1530–1534.

782 Müller, M. *et al.* (2017) "De novo transcriptome assembly and analysis of differential gene
783 expression in response to drought in European beech," *PloS one*, 12(9), p. e0184167.

784 Nelson, E. A. and Sage, R. F. (2008) "Functional constraints of CAM leaf anatomy: tight cell
785 packing is associated with increased CAM function across a gradient of CAM expression,"
786 *Journal of experimental botany*, 59(7), pp. 1841–1850.

787 Nelson, E. A., Sage, T. L. and Sage, R. F. (2005) "Functional leaf anatomy of plants with
788 crassulacean acid metabolism," *Functional plant biology: FPB*, 32(5), pp. 409–419.

789 Nowak, E. J. and Martin, C. E. (1997) "Physiological and Anatomical Responses to Water
790 Deficits in the Cam Epiphyte Tillandsia ionantha (Bromeliaceae)," *International journal of plant*
791 *sciences*. The University of Chicago Press, 158(6), pp. 818–826.

792 Nowak, M. A. *et al.* (1997) "Evolution of genetic redundancy," *Nature*, 388(6638), pp. 167–171.

793 Ogburn, R. M. and Edwards, E. J. (2009) "Anatomical variation in Cactaceae and relatives: Trait
794 lability and evolutionary innovation," *American journal of botany*, 96(2), pp. 391–408.

795 Ohrui, T. *et al.* (2007) "Foliar trichome- and aquaporin-aided water uptake in a drought-resistant
796 epiphyte Tillandsia ionantha Planchon," *Planta*, 227(1), pp. 47–56.

797 Osmond, C. B. (1978) "Crassulacean Acid Metabolism: A Curiosity in Context," *Annual review*
798 *of plant physiology*. Annual Reviews, 29(1), pp. 379–414.

799 Pierce, S., Winter, K. and Griffiths, H. (2002) "Carbon isotope ratio and the extent of daily CAM
800 use by Bromeliaceae," *The New phytologist*. Wiley, 156(1), pp. 75–83.

801 Quezada, I. M. and Gianoli, E. (2011) "Crassulacean acid metabolism photosynthesis in
802 Bromeliaceae: an evolutionary key innovation," *Biological journal of the Linnean Society.*
803 *Linnean Society of London*. Oxford Academic, 104(2), pp. 480–486.

804 Robinson, M. D., McCarthy, D. J. and Smyth, G. K. (2009) "edgeR: A Bioconductor package for
805 differential expression analysis of digital gene expression data," *Bioinformatics* . Oxford
806 University Press, 26(1), pp. 139–140.

807 Robinson, M. D. and Oshlack, A. (2010) "A scaling normalization method for differential
808 expression analysis of RNA-seq data," *Genome biology*, 11(3), p. R25.

809 Schubert, M., Lindgreen, S. and Orlando, L. (2016) "AdapterRemoval v2: rapid adapter
810 trimming, identification, and read merging," *BMC research notes*. BioMed Central, 9(1), p. 88.

811 Silvera, K. *et al.* (2009) "Crassulacean acid metabolism and epiphytism linked to adaptive
812 radiations in the Orchidaceae," *Plant physiology*, 149(4), pp. 1838–1847.

813 Silvera, K., Santiago, L. S. and Winter, K. (2005) "Distribution of crassulacean acid metabolism
814 in orchids of Panama: evidence of selection for weak and strong modes," *Functional plant*
815 *biology: FPB*, 32(5), pp. 397–407.

816 Steiner, C. C. *et al.* (2009) "The genetic basis of phenotypic convergence in beach mice: similar
817 pigment patterns but different genes," *Molecular biology and evolution*, 26(1), pp. 35–45.

818 Stiles, K. C. and Martin, C. E. (1996) "Effects of drought stress on CO2 exchange and water
819 relations in the CAM epiphyte Tillandsia utriculata (Bromeliaceae)," *Journal of plant*
820 *physiology*, 149(6), pp. 721–728.

821 Vahisalu, T. *et al.* (2008) "SLAC1 is required for plant guard cell S-type anion channel function
822 in stomatal signalling," *Nature*, 452(7186), pp. 487–491.

823 Wang, M., Zhao, Y. and Zhang, B. (2015) "Efficient Test and Visualization of Multi-Set
824 Intersections," *Scientific reports*, 5, p. 16923.

825 Wasternack, C. (2014) "Action of jasmonates in plant stress responses and development--applied
826 aspects," *Biotechnology advances*, 32(1), pp. 31–39.

827 Wickell, D. *et al.* (2021) "Underwater CAM photosynthesis elucidated by Isoetes genome,"
828 *Nature Communications 2021 12:1*. Nature Publishing Group, 12(1), pp. 1–13.

829 Winter, K. and Holtum, J. A. M. (2002) "How closely do the delta(13)C values of Crassulacean
830 Acid metabolism plants reflect the proportion of CO(2) fixed during day and night?," *Plant*
831 *physiology*, 129(4), pp. 1843–1851.

832 Yardeni, G. *et al.* (2021) "Taxon-specific or universal? Using target capture to study the
833 evolutionary history of rapid radiations," *Molecular ecology resources*. doi: 10.1111/1755-
834 0998.13523.

835 Yardeni, G. *et al.* (2023) "The explosive radiation of the Neotropical Tillandsia subgenus
836 Tillandsia (Bromeliaceae) has been facilitated by pervasive hybridization," *bioRxiv*. doi:
837 10.1101/2023.11.16.567341.

838 Yeaman, S. *et al.* (2016) "Convergent local adaptation to climate in distantly related conifers,"
839 *Science*, 353(6306), pp. 1431–1433.

840 Zhu, J.-K. (2002) "Salt and drought stress signal transduction in plants," *Annual review of plant*
841 *biology*, 53, pp. 247–273.

842

843

844

845

846

847 **11. Supporting information**

848

849 Figure S1: Diagnostic plots for Linear Mixed-Effects Models constructed in each species to assess
850 the effect of time and watering regime on titratable acidity measurements.
851 Figure S2: Mapping rates of across 24 samples of different species and watering regimes.
852 Figure S3: Principal component analysis of TMM-normalised read counts in log(CPM).
853 Figure S4: Transcript abundance in "Transcripts per Million" (TPM) for a subset of CAM-related
854 genes in T. vanhyningii (left panel) and T. leiboldiana (right panel) at two timepoints and watering
855 regimes.
856 Figure S5: Gene trees of PPC1 (A) and PPC2 (B).
857 Figure S6: Gene trees of PPCK with the isozymes PPCK1 and PPCK2.
858 Table S1: Sampling overview and summary of RNA extractions for 24 samples.
859 Table S2: Titratable acidity measurements for Tillandsia vanhyningii and Tillandsia leiboldiana at
860 four timepoints spread over 6-hour intervals.
861 Table S3: Statistical models and results for titratable acidity measurements.
862 Table S4: Summary of per-gene read counting with FeatureCounts.
863 Table S5: Statistical results of the hypergeometric test of overlaps in DE genes between species
864 and conditions
865 Table S6: Overlap of DE genes betwen species, watering regimes and time points.
866 Table S7: Description of CAM genes in sections of the Venn diagram A (Day vs Night).
867 Table S8: Description of CAM genes in sections of the Venn diagram A (Drought vs Control).